

MOL #83428

High throughput screening of small molecules identifies hepcidin antagonists

Eileen Fung, Priscilla Sugianto, Jason Hsu, Robert Damoiseaux, Tomas Ganz and Elizabeta Nemeth

Department of Medicine (EF, PS, JH, TG, EN), Department of Pathology (TG), and California

Nanosystems Institute (RD), David Geffen School of Medicine, University of California, Los Angeles,

CA, USA

MOL #83428

Running title: Identification of hepcidin antagonists

Corresponding author: Elizabeta Nemeth, UCLA David Geffen School of Medicine, 10833 LeConte Ave, CHS 37-131, Los Angeles, CA 90095, USA; Tel: 310-825-7499; E-mail:

enemeth@mednet.ucla.edu

Document statistics

Number of text pages: 31

Number of Tables: 0

Number of Figures: 6

Number of references: 33

Number of words in the Abstract: 249

Number of words in Introduction: 566

Number of words in Discussion: 686

List of nonstandard abbreviations:

FDA = Food and Drug Administration

AI = anemia of inflammation

Epo = erythropoietin

ESA = erythropoiesis stimulating agents

Fpn = ferroportin

GFP = green fluorescent protein

HTS = high-throughput screen

ELISA = Enzyme-linked immunosorbent assay

LDL = low-density lipoprotein

LDLR = low-density lipoprotein receptor

MOL #83428

HRP = horseradish peroxidase

CDD = Collaborative Drug Discovery

NAC = N-acetylcysteine (NAC)

MESNA = sodium 2-sulfanylethanesulfonate

MOL #83428

ABSTRACT

Anemia of inflammation (AI) is common in patients with infections, autoimmune diseases, cancer, and chronic kidney disease. Unless the underlying condition can be reversed, treatment options are limited to erythropoiesis-stimulating agents with or without intravenous iron therapy, modalities which are not always effective and can cause serious side effects. Hepcidin, the iron regulatory hormone, has been identified as a pathogenic factor in the development of AI. To explore new therapeutic options for AI and other iron-related disorders caused by hepcidin excess, we developed a cell-based screen to identify hepcidin antagonists. Of the 70,000 small molecules in the library, we identified 14 compounds that antagonized the hepcidin effect on ferroportin. One of these was fursultiamine, an FDA-approved thiamine derivative. Fursultiamine directly interfered with hepcidin binding to its receptor, ferroportin, by blocking ferroportin C326 thiol residue essential for hepcidin binding. Consequently fursultiamine prevented hepcidin-induced ferroportin ubiquitination, endocytosis and degradation *in vitro*, and allowed continuous cellular iron export despite the presence of hepcidin, with IC₅₀ in the sub-micromolar range. Thiamine, the fursultiamine metabolite, and benfotiamine, another thiamine derivative, did not interfere with the effect of hepcidin on ferroportin. Other FDA-approved thiol-reactive compounds were at least 1000-fold less potent than fursultiamine in antagonizing hepcidin. *In vivo*, fursultiamine did not reproducibly antagonize the effect of hepcidin on serum iron, likely due to its rapid conversion to inactive metabolites. Fursultiamine is a unique antagonist of hepcidin *in vitro* that could serve as a template for the development of drug candidates that inhibit the hepcidin-ferroportin interaction.

INTRODUCTION

Anemia of inflammation (AI, also known as anemia of chronic disease) is a condition commonly associated with chronic inflammatory disorders, including infections, inflammatory bowel diseases, rheumatoid arthritis, cancer, and chronic kidney diseases (Weiss and Goodnough, 2005). Inflammation-induced anemia is typically a mild to moderate normocytic normochromic anemia associated with hypoferremia, sequestration of iron in tissue macrophages, and a blunted response to erythropoietin (Epo). In addition, the life span of red blood cells may be shortened. If chronic, the anemia can eventually become microcytic and hypochromic (Cartwright, 1966).

Increased production of hepcidin may contribute to the development of AI. Hepcidin, a 25 amino acid peptide produced by the liver, regulates body iron concentration and distribution (Ganz and Nemeth, 2011). Hepcidin rapidly inhibits iron delivery to plasma by causing the degradation of its receptor ferroportin (SLC40A1) (Nemeth et al., 2004b). Ferroportin is the only known conduit for the delivery of cellular iron to plasma and is highly expressed in enterocytes which absorb dietary iron, macrophages which recycle iron from senescent erythrocytes, and hepatocytes which are a major iron storage site (Donovan et al., 2005; Zhang et al., 2012). Hepcidin binding to ferroportin triggers ubiquitination of multiple ferroportin lysine residues (Qiao et al., 2012) leading to the endocytosis of ferroportin and its degradation in lysosomes (Nemeth et al., 2004b), thereby blocking the iron supply to the plasma. Hepcidin-ferroportin binding involves the interaction of several aromatic residues and an unusual thiol-disulfide interaction between ferroportin cysteine thiol C326 and the hepcidin disulfide cage (Fernandes et al., 2009; Preza et al., 2011).

When hepcidin is produced in excess, the decrease of iron concentration in blood plasma leads to restriction of iron delivery to erythrocyte precursors, limiting hemoglobin synthesis. Hepcidin synthesis by hepatocytes is rapidly increased by interleukin-6 (Nemeth et al., 2004a) and other cytokines, including bone morphogenetic protein-2 (Maes et al., 2010) and activin B (Besson-Fournier et al., 2012).

MOL #83428

Accumulated evidence strongly supports the role of hepcidin as a key mediator in AI (Ganz and Nemeth, 2011). Elevated hepcidin levels have been documented in patients with chronic inflammatory conditions, in infections and sepsis, in chronic kidney diseases and in malignancies including ovarian cancer, multiple myeloma, and hepcidin-producing adenomas. In renal failure, decreased clearance of hepcidin may independently contribute to elevated hepcidin concentrations in blood (Zaritsky et al., 2009). Increased hepcidin is also seen in iron-refractory iron deficiency anemia, a genetic disorder caused by the mutations in the negative regulator of hepcidin, TMPRSS-6 (Finberg et al., 2008). Mice with increased hepcidin expression manifest resistance to erythropoietin (Roy et al., 2007; Sasu et al., 2010). In animal models of AI, interventions that targeted hepcidin or the regulators of its synthesis have improved anemia (Sasu et al., 2010; Theurl et al., 2011).

Current therapeutic options for patients with AI include relatively high doses of erythropoiesis-stimulating agents (ESAs) with or without high doses of intravenous iron (Goodnough et al., 2010). However, ESA treatments can have serious adverse effects (Glaspy, 2012), and the long term effects of high dose iron therapy are not yet known. Targeting the hepcidin-ferroportin axis could therefore improve the treatment of patients with AI.

In this study, we report the design and the results of the first high-throughput small molecule screen with the primary goal of identify hepcidin antagonists. We found 2 distinct classes of small molecules acting as hepcidin antagonists, and characterized in detail the mechanism by which an FDA-approved drug fursultiamine antagonizes the hepcidin-ferroportin axis.

MATERIALS AND METHODS

Cell culture. The EcR:Fpn-GFP cell line (Nemeth et al., 2004b) was maintained in growth medium that consisted of OptiMEM phenol red-free (Gibco, Life Technologies, Grand Island, NY), 4% fetal bovine serum (Hyclone, Thermo Fisher Scientific, Logan, UT), 200 µg/ml G418, 200 µg/ml Zeocin, 10 µg/ml

MOL #83428

ciprofloxacin, and 1% Pen/strep (Invitrogen, Life Technologies). Ponasterone (10 μ M, AG Scientific, San Diego, CA) was used to induce Fpn-GFP expression. Cells were passaged approximately every two days and were kept below 80% confluency, and were only used up to the twelfth passage.

Chemical libraries. Chemical libraries were prepared by the Molecular Shared Screening Resource (MSSR) core facility at University of California, Los Angeles. Around 70,000 small molecules from multiple libraries were screened including the Enzo Life Sciences bioactive compound library (bioactive lipids, endocannabinoids, ion channel ligands, kinase and phosphatase inhibitors, orphan receptor ligands, ~500 compounds), the Prestwick library (>1000 FDA-approved compounds), the Microsource Spectrum Collection (~2000 compounds), the ChemBridge DiverSet (~30,000 compounds) and others.

Development of the high-throughput screen (HTS) assay for hepcidin antagonist. HTS was performed at the MSSR core facility. The scheme describing the HTS assay is shown in the Supplemental Figure 1. The EcR:Fpn-GFP cells were treated with ponasterone to induce the cell-surface expression of Fpn-GFP. Addition of hepcidin causes a decrease in fluorescence due to the degradation of Fpn-GFP. The goal of the screen was to identify compounds which prevent internalization of Fpn-GFP in the presence of hepcidin, restoring the cell-surface fluorescence (hit).

To develop the HTS assay, we followed the recommendations of the NIH assay guide V4.1. (http://www.ncgc.nih.gov/guidance/manual_toc.html). Plate uniformity assessment was performed to ensure the absence of systematic sources of variability such as drifts or edge effects. Inter-plate and inter-day variability were within the acceptable range. The quality of the assay was determined by the Z' factor, a statistical measure reflective of both the signal dynamic range and the data variation within the control groups (Zhang et al., 1999). Z' is calculated as follows: $Z' = 1 - \frac{3\sigma_{c+} + 3\sigma_{c-}}{|\mu_{c+} - \mu_{c-}|}$, where μ_{c+} and μ_{c-} are means of the positive control signal and the negative control signal, and σ_{c+} and σ_{c-} are respective standard deviations. Ponasterone-induced cells (high fluorescence) were used as the positive control and hepcidin-treated cells (low fluorescence) as the negative control.

MOL #83428

Poly-D-lysine 384-well black wall/clear bottom plates (BD Biosciences, San Jose, CA) were used for screening. In each plate, 32 wells were used as positive controls (ponasterone only), 32 wells were used as negative controls (hepcidin-treated), and the center 320 wells were used for compound testing. EcR:Fpn-GFP cells were plated at a density of 8×10^4 cells/ml (4000 cell per well) using a Multidrop 384 (Thermo Scientific) and were allowed to adhere in growth medium containing 20 μ M ferric ammonium citrate (FAC) for 24 h. Ponasterone was added to all wells for the induction of Fpn-GFP expression for 18 h. The plate was washed using ELx 405 plate washer (Bio-Tek Instruments, Winooski, VT) to remove residue ponasterone and growth medium was added back to the cells. For all the wells except for the wells designated as positive controls, 50 ng/ml hepcidin (Peptides International, Louisville, KY) was added to all of the remaining 352 wells. The hepcidin concentration was selected based on the dose-response study (Figure 1A) where 50 ng/ml hepcidin nearly maximally degraded Fpn-GFP (~90%), and was close to the steep portion of the dose-response curve, allowing a marked increase in fluorescence in response to inhibitors. Test wells received compounds using a Biomek FX (Beckman Coulter, Brea, CA) with a 500 nL custom pin tool (V&P Scientific, San Diego, CA) at a target concentration of 10 μ M with a maximal DMSO concentration of 1%. DMSO was used as the solvent for compound addition. DMSO was also added to the positive and negative wells to the same final concentration. 24 h after addition of hepcidin and compounds, nuclei were stained with Hoechst 33342 DNA stain (Invitrogen), added by the automated dispenser.

Well images were acquired using high-throughput epifluorescence microscope (ImageXpress, Molecular Devices, Sunnyvale, CA) with extra long working distance 10X objective. Images were analyzed with the Multi-Wavelength Scoring Module of the ImageXpress software platform for data-mining using the GFP intensity of the cells. GFP intensity measurements per plate were transferred to Microsoft Excel where a macro was created to calculate the z' -statistic for each plate. Only plates with $z' > 0.3$ were accepted. All wells with high GFP signal were also visually inspected to account for the cellular localization of Fpn-

MOL #83428

GFP. Wells were rated categorically on a three-point scale: (1) Fpn-GFP clearly on the membrane, (2) no changes in the morphology of the cells, and (3) viability of cells.

The small molecules considered as preliminary hits were additionally screened in triplicates for confirmation (cherry-picking). The confirmed hits were then tested in a dose-dependent manner to calculate the IC₅₀.

Ferritin measurements. Cellular protein was extracted with RIPA buffer (Boston BioProducts, Ashland, MA) and a protease inhibitor cocktail (Roche, Indianapolis, IN). Ferritin levels were determined by an enzyme-linked immunosorbent assay (ELISA) assay (Ramco Laboratories, Stafford, TX) according to the manufacturer's instructions and were normalized for the total protein concentration in each sample. Total protein concentration was determined by the bicinchoninic acid (BCA) assay (Pierce, Rockford, IL).

Flow cytometry. Flow cytometry was performed as previously described (Nemeth et al., 2006). EcR:Fpn-GFP cells were incubated with or without 10 μM ponasterone for 24 h. After three washes with 1xDPBS, the cells were treated with hepcidin along with small molecules or solvent for another 24 h. Cells were detached using TrypLE Express (Invitrogen) and resuspended in medium at 1x10⁶ cells/mL. The intensity of green fluorescence was measured by flow cytometry at the UCLA Jonsson Comprehensive Cancer Center (JCCC) and Center for AIDS Research Flow Cytometry Core Facility that is supported by National Institutes of Health awards CA-16042 and AI-28697, and by the JCCC, the UCLA AIDS Institute, and the David Geffen School of Medicine at UCLA. Cells not expressing Fpn-GFP (no ponasterone) were used to establish a gate to exclude background fluorescence. Each treatment was repeated independently at least 3 times. The results were represented as a fraction of the GFP intensity of untreated cells, according to the formula $(F_x - F_{\text{hep}}) / (F_{\text{untreated}} - F_{\text{hep}})$, where F represents the mean of the gated green fluorescence.

Immunoprecipitation and Western blotting. Cell lysis, immunoprecipitation, and Western blotting were performed as previously described (Qiao et al., 2012). Polyclonal anti-GFP antibody (ab290,

MOL #83428

Abcam, Cambridge, MA) was used for immunoprecipitation, biotinylated proteins were detected with streptavidin-HRPO (Pierce), and either a monoclonal anti-mouse GFP (clone 13.1, Roche) or rat anti-mouse Fpn antibody R1 (Qiao et al., 2012) was used to determine the amount of ferroportin-GFP that was immunoprecipitated.

Cell surface biotinylation. EcR:Fpn-GFP cells were induced to express Fpn-GFP for 18 h. Following the removal of the inducing agent, the cells were treated with either hepcidin or selected small molecules for 30 minutes. Cells were rinsed with PBS and treated with 50 μ M nonpermeable thiol-reactive biotinylation reagent (maleimide-PEG₂-biotin, Pierce) or nonpermeable primary amine-reactive biotinylation reagent (NHS-PEG₂-biotin, Pierce) for 30 minutes at 4°C in a rotary shaker. The reagent was washed off with PBS, total protein was isolated and immunoprecipitated with anti-GFP antibody (Abcam), and blotted using streptavidin-horseradish peroxidase (HRPO, Pierce) for the detection of biotinylated species.

¹²⁵I-hepcidin uptake assay. ¹²⁵I-hepcidin was prepared as previously described (Nemeth et al., 2004b), and 10⁶ cpm/ml added to EcR:Fpn-GFP cells for 1 hour at 37°C. To remove unbound radioactive hepcidin, the cells were washed with PBS 3 times and centrifuged for 2 minutes at 12,000xg through a silicone oil layer (Nyosil M25; Nye). The radioactivity in the cell pellets was determined by gamma counting. The data were expressed as a fraction of the radioactivity of induced Fpn-GFP cells (positive control), with the radioactivity of uninduced cells subtracted as background for each condition.

Biotin-hepcidin binding assay. Cells were induced with ponasterone to express Fpn-GFP for 18 h. Following the removal of the inducing agent, cells were treated with 2.5, 5, and 10 μ g/ml N-terminally biotinylated hepcidin (Peptides International, Louisville, KY) for 30 min at 37°C. Protein lysates were harvested and immediately immunoprecipitated with anti-GFP antibody. We then used Streptavidin-HRP (Pierce) to detect biotin-hepcidin.

LDLR-internalization assay. EcR:Fpn-GFP cells were incubated 12 h in 1% FBS, simvastatin, and mevalonic acid to increase the expression of endogenous LDLR. Small molecules, hepcidin and GW3965

MOL #83428

were added to the medium for additional 16 h. GW3965 is an LXR agonist which prevents internalization of LDL by LDLR (Zelcer et al., 2009), and was provided by Dr. Peter Tontonoz, UCLA. To measure LDL uptake, fluorescent DiI-LDL (2.5 $\mu\text{g/mL}$, Invitrogen, Eugene, OR) was added for 30 minutes at 37°C. The cells were washed with dPBS containing 0.2% bovine serum albumin (BSA) and lysed in RIPA supplemented with protease inhibitors and phenylmethylsulfonyl fluoride (PMSF) (Sigma). Cell lysates were collected and cleared by centrifugation, and 30 μL aliquots were loaded in a 384-well plate. Fluorescent LDL was quantified with a Typhoon scanner (GE Healthcare, Pittsburgh, PA) at an excitation wavelength of 554 nm and an emission wavelength of 571 nm. Total cellular protein was measured using BCA assay, and fluorescence units were normalized to total protein.

In vivo serum iron measurement. Six weeks old male C57BL/6 mice were fed a diet with decreased iron content (20 ppm) for 1 week. This regimen lowers endogenous hepcidin expression and increases animal responsiveness to synthetic hepcidin injection (Rivera et al., 2005). Mice (n=4 per group) were injected intraperitoneally first with 0.5-2.5 mg fursultiamine (AK Scientific, Union City, CA), then after 1 h with 50 μg hepcidin (Peptides International). In another experiment, three doses of fursultiamine (2.5 mg/injection) were administered over 24 h, followed by hepcidin injection 1 h after the last dose. Serum iron was measured 3 h after hepcidin injection using a colorimetric method (Nemeth et al., 2004a). The selected doses of fursultiamine were 5-25-fold below the reported LD50 dose for intraperitoneal administration of fursultiamine in mice (540 mg/kg) (TAKHAA Takeda Kenkyusho Ho, 1971). Thiamine concentration measurements were performed at Antech Diagnostics (Irvine, CA).

Statistics. We used SigmaStat 11 for statistical analyses (Systat Software, Point Richmond, CA). Normally distributed data were compared using t-test. Measurements that were not normally distributed were compared by the nonparametric Mann-Whitney rank sum test. $P < 0.05$ was considered statistically significant. For in vivo experiments, we used 4 mice per treatment group based on the following consideration. A therapeutically meaningful effect of fursultiamine would be to increase serum iron by 10

MOL #83428

μM or more. A typical standard deviation in our experiments is around 3 μM . With $p=0.05$ and $n=4$ mice per group, a power of 0.9 would be expected.

RESULTS

Developing a small molecule high-throughput screen for hepcidin antagonists. We used the HEK293T cell line expressing an inducible ferroportin (Fpn)-GFP construct (Nemeth et al., 2004b) to identify small molecules that prevent Fpn-GFP internalization in the presence of hepcidin (the screening scheme is depicted in Supplemental Figure 1). We opted for high-content screening approach using a high-throughput epifluorescence microscope and image analysis software, which allowed us to screen not only by quantifying the Fpn-GFP signal but also by the cellular localization of Fpn-GFP. This was important in order to eliminate compounds which only interfered with ferroportin degradation but not its internalization, as those would not restore cellular iron export. The development of the assay included determination of the optimal concentration of hepcidin (Figure 1A) and cellular density (Supplemental Table 1) based on the z-statistics (Zhang et al., 1999). The final screen was performed using a 24 h incubation time-point with 50 ng/ml hepcidin and 10 μM concentration of small molecules (~70,000 compounds). Initially, 2.642% compounds were identified as preliminary hits based solely on the high intensity of GFP (arbitrarily chosen as $\geq 60\%$ of the fluorescence of hepcidin-untreated cells, Figure 1B). We then visually inspected the images to select the primary hits which prevented ferroportin endocytosis in the presence of hepcidin (Figure 1C), and to delete from the hit list those compounds that only prevented Fpn-GFP degradation but not internalization, and compounds with auto fluorescence. The triplicate retesting of selected primary hits confirmed 2 chemically distinct groups of small molecules as hepcidin antagonists. One group of compounds (A1 – A8, Figure 1C) were cardiac glycosides which share a characteristic steroid backbone. Some of these small molecules have been used to treat chronic heart failure and atrial arrhythmias (Ehle et al., 2011). Interestingly, only nanomolar concentrations of cardiac glycosides were needed to prevent the internalization of ferroportin. These concentrations are

MOL #83428

much lower than those known to cause adverse side effects (Ehle et al., 2011). The mechanism by which cardiac glycosides antagonize hepcidin is the subject of a separate study and these compounds will not be further discussed in the manuscript.

The second group of small molecules identified as hepcidin antagonists (B1: fursultiamine hydrochloride, B2: thioxolone, and B3: pyrithione zinc) were all FDA-approved compounds that contain a sulfur moiety with potential thiol-directed chemical reactivity. This set of molecules was of particular interest since we previously showed that hepcidin-ferroportin binding may involve a thiol-disulfide interaction (Fernandes et al., 2009;Preza et al., 2011). Dose response curves generated using the high-throughput microscope and image analysis software showed that in the presence of 50 ng/ml hepcidin, these compounds prevented Fpn-GFP degradation with IC₅₀ concentrations of 0.094 μM (fursultiamine hydrochloride), 0.002 μM (pyrithione zinc), and 1.98 μM (thioxolone) (Figure 2A).

The effect of HTS hits on hepcidin-mediated ferroportin degradation and cellular iron export. To further validate fursultiamine hydrochloride, thioxolone and pyrithione zinc as hepcidin antagonists, we quantitated their effect on the degradation of Fpn-GFP by flow cytometry. Fpn-GFP cells were treated for 24 h with 100 ng/ml hepcidin with and without the compounds (10 μM). All three compounds antagonized the effect of hepcidin and prevented Fpn-GFP degradation (Figure 2B), although pyrithione zinc showed significant toxicity and caused cell death. Interestingly, cells treated with fursultiamine retained more Fpn-GFP than untreated cells suggesting that fursultiamine may prevent Fpn-GFP turnover.

We next investigated the compounds' effect on iron-exporting function of ferroportin. Fpn-GFP cells were treated for 24 h with 100 ng/ml hepcidin and 10 μM compounds, and intracellular iron concentrations were assessed using ferritin ELISA. Pyrithione zinc at 10 μM consistently caused cellular toxicity after 24 h treatment so only data for fursultiamine and thioxolone are shown. As expected, induction of Fpn-GFP with ponasterone caused a decrease in ferritin levels whereas hepcidin addition reversed this effect causing iron retention and an increase in ferritin (Figure 2C). When fursultiamine was added together

MOL #83428

with hepcidin, it completely blocked the effect of hepcidin and lowered intracellular ferritin to the levels seen in ponasterone-induced cells. Thioxolone was much less potent in antagonizing hepcidin and only had a minor effect on reducing intracellular ferritin. Western blotting of the total cellular protein confirmed that fursultiamine and to a lesser extent thioxolone treatment was able to prevent hepcidin-mediated degradation of ferroportin (Figure 2C).

Hepcidin Antagonists: Mode of Action. Antagonists may prevent hepcidin-mediated ferroportin internalization by at least three distinct mechanisms: 1) preventing the interaction between hepcidin and ferroportin; 2) inhibiting hepcidin-induced ubiquitination of ferroportin; and 3) inhibiting the endocytosis pathway for ferroportin internalization. We hypothesized that the three hits with potential thiol reactivity prevented hepcidin binding to ferroportin by blocking the critical C326 thiol residue on ferroportin. To assess the binding of hepcidin to ferroportin, we treated Fpn-GFP expressing cells with radiolabeled ^{125}I -hepcidin and putative antagonists (10 μM) for 1 h, and monitored cell-associated ^{125}I -hepcidin. Because of the short duration of the experiment, pyrithione zinc was well tolerated. In comparison to control cells (solvent-treated), fursultiamine and pyrithione zinc but not thioxolone treatment significantly decreased ^{125}I -hepcidin uptake (Figure 2D). The results indicate that fursultiamine and pyrithione zinc interfered with the hepcidin-ferroportin interaction that is necessary for ferroportin endocytosis and iron retention.

Of the three FDA-approved, potentially thiol-reactive compounds, fursultiamine showed the most desirable characteristics as hepcidin antagonist *in vitro*: it potently prevented hepcidin-mediated ferroportin degradation and restored iron export in the presence of hepcidin. The other two compounds were less effective. Although pyrithione zinc mode of action appeared to be similar to that of fursultiamine (blocking of hepcidin binding to ferroportin), it had significant cellular toxicity with prolonged treatment duration, whereas thioxolone failed to promote iron export in the presence of hepcidin and only prevented ferroportin degradation. Therefore, our subsequent analyses were focused on fursultiamine.

Fursultiamine inhibits hepcidin-induced internalization of ferroportin and promotes cellular iron

export. To fully characterize fursultiamine as a hepcidin antagonist, we examined its dose-dependent effect on cellular iron export. Fpn-GFP cells were treated with 100 ng/ml hepcidin and 0-50 μ M fursultiamine for 24 h, and intracellular ferritin concentration determined (Figure 3A). Fursultiamine reversed the effect of hepcidin on ferritin levels, with the IC₅₀ dose in the sub-micromolar range. To confirm that ferroportin is indeed retained on the plasma membrane when treated with fursultiamine, we performed a cell surface biotinylation assay using primary amine-reactive biotin followed by an immunoprecipitation of cell lysates with an anti-GFP antibody. Immunoblotting with streptavidin to detect biotinylated Fpn-GFP demonstrated that even in the presence of hepcidin, fursultiamine-treated cells retained ferroportin on the plasma membrane in a dose-dependent manner (Figure 3B). Retention of Fpn-GFP on the membrane despite the presence of hepcidin should also manifest as decreased Fpn-GFP degradation. Western blotting of total cellular protein confirmed that overnight treatment with fursultiamine prevented hepcidin-induced Fpn-GFP degradation, and this was also seen at a higher hepcidin dose (100 vs 250 ng/ml hepcidin, Figure 3C).

Fursultiamine prevents hepcidin-induced posttranslation modification of ferroportin.

The interaction between hepcidin and ferroportin leads to rapid ubiquitination of ferroportin which triggers ferroportin endocytosis (Qiao et al., 2012). Since fursultiamine prevents hepcidin-mediated endocytosis of ferroportin, we hypothesized that fursultiamine may prevent ferroportin ubiquitination. Fpn-GFP expressing cells were treated with 1 μ g/ml hepcidin and increasing doses of fursultiamine, cell lysates were immunoprecipitated with anti-GFP antibody and Fpn-GFP ubiquitination detected using an antibody against mono/poly-ubiquitin (Figure 3D). Fursultiamine decreased ferroportin ubiquitination in a dose-dependent manner, confirming that the antagonist acts upstream of ligand-induced ubiquitination of ferroportin.

Fursultiamine does not inhibit the endocytosis of LDL receptor.

We next sought to address the specificity of fursultiamine for ferroportin by testing its effect on endocytosis of another receptor. We

MOL #83428

chose low density lipid (LDL) receptor because it is ubiquitously expressed in most cell types and its endocytosis is also ligand-induced (cholesterol-rich LDL). Figure 3E shows that increasing dosage of fursultiamine had no effect on the uptake of fluorescent LDL by LDLR. As a control, cells were also treated with a liver X receptor agonist (GW3965), a known inhibitor of the LDL uptake by LDLR (Zelcer et al., 2009). This result indicates that fursultiamine does not cause a general inhibition of endocytosis pathways.

Fursultiamine tightly associates with ferroportin. Earlier in the study, we reported that fursultiamine prevented association of ¹²⁵I-hepcidin with cells expressing Fpn-GFP (Figure 2D). To assess whether fursultiamine irreversibly blocks ferroportin interaction with hepcidin, we pre-treated Fpn-GFP cells with fursultiamine for 30 minutes, then in one set of cells removed fursultiamine by thoroughly rinsing the cells 3 times with DPBS (pre-treatment or "Pre-T"), and in another set of cells left fursultiamine in the cell media (co-treatment or "Co-T"). Hecpidin was then added to all the cells for 1 or 2 h and Fpn-GFP measured by flow cytometry (Figure 4A). Hecpidin by itself caused Fpn-GFP degradation, whereas both pre-treatment and co-treatment of Fpn-GFP cells with fursultiamine prevented hepcidin-induced Fpn-GFP degradation. This indicates that interaction of fursultiamine with ferroportin is sufficient for hepcidin antagonism, and that fursultiamine remains associated with ferroportin despite washing, possibly because of a formation of a covalent bond.

Hecpidin binding to ferroportin is attenuated in the presence of fursultiamine. To confirm that fursultiamine interferes with hepcidin binding to ferroportin, we assessed the binding of increasing concentrations of biotinylated hepcidin (2.5 – 10 µg/ml) to cells expressing Fpn-GFP in the absence or presence of fursultiamine (10 µM) (Figure 4B). Cell lysates were immunoprecipitated with anti-GFP antibody and association of biotin-hepcidin with ferroportin visualized by immunoblotting using streptavidin-HRP. Fursultiamine interfered with hepcidin binding to ferroportin at the two lower biotin-hepcidin doses, and was outcompeted only by the highest concentration of biotin-tagged hepcidin. The

data also indicate that very high concentrations of hepcidin can reverse the inhibition of hepcidin binding after pretreatment by fursultiamine.

Our group had previously identified that an extracellular ferroportin thiol-cysteine residue (C326) is essential for hepcidin binding (Fernandes et al., 2009). C326-SH can be specifically biotinylated using maleimide-biotin reagent (Fernandes et al., 2009;Preza et al., 2011), and this biotinylation is prevented in the presence of hepcidin (Figure 4C). To assess if fursultiamine antagonizes hepcidin by blocking the C326 residue on ferroportin, we treated cells expressing Fpn-GFP with either hepcidin or fursultiamine followed by the maleimide-biotin reagent. Both hepcidin and fursultiamine decreased thiol-specific biotinylation of Fpn-GFP in a dose-dependent manner (Figure 4C). This suggests that fursultiamine, like hepcidin, interacts with C326 residue on ferroportin. We cannot, however, completely exclude the possibility that fursultiamine indirectly blocks access to C326 by reacting with another residue on ferroportin.

Metabolites or congeners of fursultiamine hydrochloride do not act as hepcidin antagonists.

Fursultiamine is a synthetic small molecule originally designed to treat thiamine deficiency (Lonsdale, 2004). Also known as thiamine disulfide, fursultiamine was designed to be more lipophilic than its natural counterpart, thiamine hydrochloride. When fursultiamine is ingested orally, the disulfide bond is cleaved by an unknown enzyme releasing thiamine into the bloodstream (Kitamori and Itokawa, 1993;Lonsdale, 2004). We thus asked whether thiamine will exert a similar effect on hepcidin-ferroportin interaction as fursultiamine. Cells expressing Fpn-GFP were treated with hepcidin and either fursultiamine (1-30 μ M) or thiamine (1-100 μ M), and Fpn-GFP levels quantified by flow cytometry. Unlike fursultiamine, thiamine did not antagonize hepcidin-induced degradation of Fpn-GFP (Figure 5A).

After thiamine is cleaved from fursultiamine, the remaining prosthetic group (tetrahydrofurfuryl mercaptane) is converted into a number of metabolites which are excreted in urine (Nishikawa et al., 1970). The metabolites of the prosthetic group are not available commercially, but we tested a related

MOL #83428

compound, furfuryl methyl sulfide. Flow cytometry of Fpn-GFP expressing cells treated with furfuryl methyl sulfide showed that the compound failed to antagonize hepcidin (Supplemental Figure 2A). Benfotiamine, a synthetic thiamine derivative lacking the labile disulfide of fursultiamine (Pan et al., 2010) also did not prevent hepcidin-mediated degradation of ferroportin (Supplemental Figure 2B).

Other thiol-modifying drugs are weak or inactive as antagonists of hepcidin. Previous studies from our group have suggested that a thiol-disulfide exchange may occur during hepcidin binding to ferroportin (Fernandes et al., 2009;Preza et al., 2011). Fursultiamine is a compound with a disulfide bond connecting thiamine to tetrahydrofurfuryl mercaptane. Our new data suggest that the disulfide bond of fursultiamine likely interacts with the ferroportin C326-thiol and as a result blocks hepcidin from docking. We searched for compounds with similar structure as fursultiamine by performing structural clustering with the compounds in the libraries of PubChem (NIH) and Collaborative Drug Discovery (CDD), but our searches demonstrated that fursultiamine has no structural homologs in these libraries. We therefore compared fursultiamine to other FDA-approved compounds with known thiol-modifying abilities: N-acetylcysteine (NAC) and sodium 2-sulfanylethanesulfonate (commonly known as MESNA). Both NAC and MESNA have antioxidant properties and are currently used as therapeutics. NAC, a derivative of cysteine, is used as an antidote for acetaminophen overdose, and has potential utility in the treatment of psychiatric disorders, chronic obstructive pulmonary disease, pulmonary fibrosis and other conditions (Millea, 2009). MESNA is an organosulfur compounds used as a cytoprotective agent to help reduce bladder toxicity caused by certain chemotherapy drugs (Hogle, 2007). Figure 5B shows the flow cytometry analysis of the effect of NAC and MESNA on hepcidin-mediated Fpn degradation. In contrast to fursultiamine which potently prevented hepcidin-induced Fpn degradation, NAC only modestly antagonized hepcidin at 1000-fold higher concentrations and MESNA did not interfere with hepcidin effect on Fpn-GFP at concentrations tested.

Fursultiamine is not a robust antagonist *in vivo*. To assess the potential of fursultiamine as a hepcidin antagonist *in vivo*, male C57BL/6 mice were injected intraperitoneally with 0.5-2.5 mg fursultiamine,

MOL #83428

followed 1h later by 50 μg hepcidin, and serum iron concentrations assessed 3 h after hepcidin injection. The fursultiamine doses were expected to yield much higher concentrations in circulation (0.6-3 mM) than the IC₅₀ we observed *in vitro* for fursultiamine (<1 μM). Although in one experiment fursultiamine reversed the effect of hepcidin on serum iron (Figure 6A), the effect was not reproducible (Figure 6B and Supplemental Figure 3). This is likely due to the very rapid degradation of fursultiamine into thiamine *in vivo* (Kitamori and Itokawa, 1993). As expected, fursultiamine administration resulted in a dramatic increase in thiamine concentrations in mouse serum within 4 h (151 $\mu\text{g}/\text{l}$ in solvent-injected mice vs 1393 $\mu\text{g}/\text{l}$ in fursultiamine-injected mice).

DISCUSSION

Anemia of inflammation is an iron disorder associated with abnormally high hepcidin. As hepcidin causes rapid removal of ferroportin from the membrane, iron is sequestered within the tissues, limiting iron availability for erythropoiesis. The use of neutralizing hepcidin antibodies or inhibitors of hepcidin expression in animal models improved or prevented development of anemia caused by an inflammatory stimulus (Sasu et al., 2010;Theurl et al., 2011) showing the potential utility of hepcidin antagonists in treating AI.

We took an unbiased approach to identify small compounds acting as hepcidin antagonists, both to inform about the mechanisms of hepcidin-induced ferroportin internalization and to develop lead compounds for the treatment of AI. In AI, the antagonism of the effect of hepcidin would promote cellular iron export in the face of elevated hepcidin concentrations, reverse the iron-restrictive effect of inflammation and make more iron available for hemoglobin synthesis. We chose high-throughput microscopy of Fpn-GFP expressing cells because this high-content screening methodology allowed us to decrease the rate of false positives and only focus on small molecules that retained ferroportin on the plasma membrane despite the presence of hepcidin.

MOL #83428

We identified 2 classes of small molecules as potential hepcidin antagonists: a group of compounds with potential thiol reactivity, and cardiac glycosides. Cardiac glycosides function by binding to Na/K ATPase and either inhibiting its activity or initiating a signal transduction cascade (Riganti et al., 2011). The role of Na/K ATPase in iron metabolism has not been described and is the subject of a separate manuscript (in preparation). The discovery of the hepcidin-antagonistic effects of three thiol-reactive molecules is consistent with our prior studies indicating that hepcidin-ferroportin binding involves interaction between C326 thiol on ferroportin and the disulfide cage of hepcidin (Fernandes et al., 2009;Preza et al., 2011). Furthermore, human mutations in the C326 residue cause complete resistance of ferroportin to hepcidin-induced endocytosis and lead to the development of severe iron overload (Sham et al., 2005). Of the three sulfur-containing compounds, fursultiamine was of the greatest interest, as the others either caused cellular toxicity with long-term treatment (pyrithione zinc) or did not reverse the inhibitory effect of hepcidin on iron export (thioxolone).

Fursultiamine is a synthetic thiamine derivative with a disulfide bond in its chemical backbone. We showed that fursultiamine blocked the C326 residue on ferroportin and prevented hepcidin from binding. Consistent with this mechanism, fursultiamine also inhibited hepcidin-induced ferroportin ubiquitination, an early signal controlling ferroportin endocytosis. Cotreatment of cells with hepcidin and fursultiamine resulted in ferroportin retention on the cell membrane and continued cellular iron export. Furthermore, the fursultiamine effect seems specific to hepcidin-ferroportin interaction as fursultiamine did not affect the endocytosis of the LDL receptor.

Interestingly, in searches of PubChem and Collaborative Drug Discovery libraries, fursultiamine seemed to possess a unique chemical structure. Other compounds that are closest to the chemical structure of fursultiamine are thiamine and other thiamine-derivatives such as benfotiamine. However, neither acted as a hepcidin antagonist. We also tested NAC and MESNA, two FDA-approved small molecules known for their thiol-modifying abilities, but these also failed to significantly antagonize the hepcidin effect on ferroportin at comparable concentrations. It is not clear why fursultiamine shows superior potency as

MOL #83428

hepcidin antagonist in comparison to other thiol-modifying molecules. Our previous study (Preza et al., 2011) demonstrated that in addition to the thiol-disulfide interaction between hepcidin and ferroportin, the ligand-receptor binding also depends on the interaction of neighboring aromatic residues. We speculate that the ring region of fursultiamine may increase the affinity of this compound for ferroportin on the cell membrane compared to other thiol-reactive molecules.

Although fursultiamine is already an FDA-approved drug, opening a possibility of “repurposing” the drug for the treatment of AI, its effects *in vitro* do not readily translate into the *in vivo* setting. Fursultiamine was designed to be an efficient replacement for thiamine. When fursultiamine is orally delivered, the drug is very rapidly (within 1 h) metabolized into thiamine (Kitamori and Itokawa, 1993). Thiamine, however, does not antagonize hepcidin-ferroportin interaction. Thus, in order for fursultiamine to be effective as a hepcidin antagonist *in vivo*, modifications of its chemistry, formulation or methods for delivery to target tissues would be necessary.

ACKNOWLEDGMENTS

We thank Dr. Peter Tontonoz for the assistance with the LDL-LDLR internalization assay.

AUTHORSHIP CONTRIBUTIONS

Participated in research design: Fung, Damoiseaux, Ganz, Nemeth

Conducted experiments: Fung, Sugianto, Hsu, Damoiseaux

Contributed reagents and analytic tools: Damoiseaux

Performed data analysis: Fung, Sugianto, Hsu, Ganz, Nemeth

Participated in the writing of the manuscript: Fung, Damoiseaux, Ganz, Nemeth

MOL #83428

Reference List

Besson-Fournier C, Latour C, Kautz L, Bertrand J, Ganz T, Roth M P and Coppin H (2012) Induction of Activin B by Inflammatory Stimuli Up-Regulates Expression of the Iron-Regulatory Peptide Heparin Through Smad1/5/8 Signaling. *Blood* **120**:431-439.

Cartwright GE (1966) The Anemia of Chronic Disorders. *Semin Hematol* **3**:351-375.

Donovan A, Lima C A, Pinkus J L, Pinkus G S, Zon L I, Robine S and Andrews N C (2005) The Iron Exporter Ferroportin/Slc40a1 Is Essential for Iron Homeostasis. *Cell Metab* **1**:191-200.

Ehle M, Patel C and Giugliano R P (2011) Digoxin: Clinical Highlights: a Review of Digoxin and Its Use in Contemporary Medicine. *Crit Pathw Cardiol* **10**:93-98.

Fernandes A, Preza G C, Phung Y, De D, I, Kaplan J, Ganz T and Nemeth E (2009) The Molecular Basis of Heparin-Resistant Hereditary Hemochromatosis. *Blood* **114**:437-443.

Finberg KE, Heeney M M, Campagna D R, Aydinok Y, Pearson H A, Hartman K R, Mayo M M, Samuel S M, Strouse J J, Markianos K, Andrews N C and Fleming M D (2008) Mutations in Tmprss6 Cause Iron-Refractory Iron Deficiency Anemia (IRIDA). *Nat Genet* **40**:569-571.

Ganz T and Nemeth E (2011) Heparin and Disorders of Iron Metabolism. *Annu Rev Med* **62**:347-360.

Glaspy J (2012) Update on Safety of ESAs in Cancer-Induced Anemia. *J Natl Compr Canc Netw* **10**:659-666.

Goodnough LT, Nemeth E and Ganz T (2010) Detection, Evaluation, and Management of Iron-Restricted Erythropoiesis. *Blood* **116**:4754-4761.

Hogle WP (2007) Cytoprotective Agents Used in the Treatment of Patients With Cancer. *Semin Oncol Nurs* **23**:213-224.

MOL #83428

Kitamori N and Itokawa Y (1993) Pharmacokinetics of Thiamin After Oral Administration of Thiamin Tetrahydrofurfuryl Disulfide to Humans. *J Nutr Sci Vitaminol (Tokyo)* **39**:465-472.

Lonsdale D (2004) Thiamine Tetrahydrofurfuryl Disulfide: a Little Known Therapeutic Agent. *Med Sci Monit* **10**:RA199-RA203.

Maes K, Nemeth E, Roodman G D, Huston A, Esteve F, Freytes C, Callander N, Katodritou E, Tussing-Humphreys L, Rivera S, Vanderkerken K, Lichtenstein A and Ganz T (2010) In Anemia of Multiple Myeloma, Heparin Is Induced by Increased Bone Morphogenetic Protein 2. *Blood* **116**:3635-3644.

Millea PJ (2009) N-Acetylcysteine: Multiple Clinical Applications. *Am Fam Physician* **80**:265-269.

Nemeth E, Preza G C, Jung C L, Kaplan J, Waring A J and Ganz T (2006) The N-Terminus of Heparin Is Essential for Its Interaction With Ferroportin: Structure-Function Study. *Blood* **107**:328-333.

Nemeth E, Rivera S, Gabayan V, Keller C, Taudorf S, Pedersen B K and Ganz T (2004a) IL-6 Mediates Hypoferremia of Inflammation by Inducing the Synthesis of the Iron Regulatory Hormone Heparin. *J Clin Invest* **113**:1271-1276.

Nemeth E, Tuttle M S, Powelson J, Vaughn M B, Donovan A, Ward D M, Ganz T and Kaplan J (2004b) Heparin Regulates Cellular Iron Efflux by Binding to Ferroportin and Inducing Its Internalization. *Science* **306**:2090-2093.

Nishikawa K, Kikuchi S and Suzuoki Z (1970) The Metabolic Fate of Methyl Tetrahydrofurfuryl Sulfide and Its Related Compounds in Rats. *Eur J Pharmacol* **9**:111-115.

Pan X, Gong N, Zhao J, Yu Z, Gu F, Chen J, Sun X, Zhao L, Yu M, Xu Z, Dong W, Qin Y, Fei G, Zhong C and Xu T L (2010) Powerful Beneficial Effects of Benfotiamine on Cognitive Impairment and Beta-Amyloid Deposition in Amyloid Precursor Protein/Presenilin-1 Transgenic Mice. *Brain* **133**:1342-1351.

MOL #83428

Preza GC, Ruchala P, Pinon R, Ramos E, Qiao B, Peralta M A, Sharma S, Waring A, Ganz T and Nemeth E (2011) Minihepcidins Are Rationally Designed Small Peptides That Mimic Heparin Activity in Mice and May Be Useful for the Treatment of Iron Overload. *J Clin Invest* **121**:4880-4888.

Qiao B, Sugianto P, Fung E, Del-Castillo-Rueda A, Moran-Jimenez M J, Ganz T and Nemeth E (2012) Heparin-Induced Endocytosis of Ferroportin Is Dependent on Ferroportin Ubiquitination. *Cell Metab* **15**:918-924.

Riganti C, Campia I, Kopecka J, Gazzano E, Doublier S, Aldieri E, Bosia A and Ghigo D (2011) Pleiotropic Effects of Cardioactive Glycosides. *Curr Med Chem* **18**:872-885.

Rivera S, Nemeth E, Gabayan V, Lopez M A, Farshidi D and Ganz T (2005) Synthetic Heparin Causes Rapid Dose-Dependent Hypoferremia and Is Concentrated in Ferroportin-Containing Organs. *Blood* **106**:2196-2199.

Roy CN, Mak H H, Akpan I, Losyev G, Zurakowski D and Andrews N C (2007) Heparin Antimicrobial Peptide Transgenic Mice Exhibit Features of the Anemia of Inflammation. *Blood* **109**:4038-4044.

Sasu BJ, Cooke K S, Arvedson T L, Plewa C, Ellison A R, Sheng J, Winters A, Juan T, Li H, Begley C G and Molineux G (2010) Anti-Heparin Antibody Treatment Modulates Iron Metabolism and Is Effective in a Mouse Model of Inflammation-Induced Anemia. *Blood*.

Sham RL, Phatak P D, West C, Lee P, Andrews C and Beutler E (2005) Autosomal Dominant Hereditary Hemochromatosis Associated With a Novel Ferroportin Mutation and Unique Clinical Features. *Blood Cells Mol Dis* **34**:157-161.

TAKHAA Takeda Kenkyusho Ho (1971) *Journal of the Takeda Research Laboratories* **30**:242.

MOL #83428

Theurl I, Schroll A, Sonnweber T, Nairz M, Theurl M, Willenbacher W, Eller K, Wolf D, Seifert M, Sun C C, Babitt J L, Hong C C, Menhall T, Gearing P, Lin H Y and Weiss G (2011) Pharmacologic Inhibition of Hcpidin Expression Reverses Anemia of Chronic Inflammation in Rats. *Blood* **118**:4977-4984.

Weiss G and Goodnough L T (2005) Anemia of Chronic Disease. *N Engl J Med* **352**:1011-1023.

Zaritsky J, Young B, Wang H J, Westerman M, Olbina G, Nemeth E, Ganz T, Rivera S, Nissenson A R and Salusky I B (2009) Hcpidin--a Potential Novel Biomarker for Iron Status in Chronic Kidney Disease. *Clin J Am Soc Nephrol* **4**:1051-1056.

Zelcer N, Hong C, Boyadjian R and Tontonoz P (2009) LXR Regulates Cholesterol Uptake Through Idol-Dependent Ubiquitination of the LDL Receptor. *Science* **325**:100-104.

Zhang JH, Chung T D and Oldenburg K R (1999) A Simple Statistical Parameter for Use in Evaluation and Validation of High Throughput Screening Assays. *J Biomol Screen* **4**:67-73.

Zhang Z, Zhang F, Guo X, An P, Tao Y and Wang F (2012) Ferroportin1 in Hepatocytes and Macrophages Is Required for the Efficient Mobilization of Body Iron Stores in Mice. *Hepatology* **56**:961-971.

MOL #83428

FOOTNOTES

The work was supported by the National Institutes of Health National Institute of Diabetes and Digestive and Kidney Diseases (grant R01 DK082717) and the UCLA Pepper Center for Aging (grant P30 AG028748).

FIGURE LEGENDS

Figure 1. Development of a small molecule high-throughput screen (HTS) for hepcidin antagonists.

A) *Effect of hepcidin concentration on Fpn-GFP degradation in the HTS assay.* EcR:Fpn-GFP cells were seeded in 384-well plates and induced with 10 μ M ponasterone for 18 h to express Fpn-GFP. Hepcidin was then added in the range of concentrations 0 – 5000 ng/ml for 24 h. Nuclei were stained with blue Hoechst 33342 dye. Images of each well were acquired with the high-throughput epifluorescence microscope (representative images are shown below the graph), and GFP fluorescence intensity determined using MetaMorph software. The results are expressed as normalized fluorescence so that cells induced with ponasterone but not treated with hepcidin had 100% Fpn-GFP content and cells treated with the highest dose of hepcidin had 0% Fpn-GFP. Each point is the mean of 3 replicates and error bars represent standard deviation. Hepcidin treatment caused degradation of Fpn-GFP in a dose dependent manner. The data points were fitted with a 4-parameter logistic curve and yielded EC₅₀ of 9 ng/ml. The red arrow indicates the concentration of hepcidin selected for the screening of small molecules. It was chosen because it nearly maximally degraded Fpn-GFP and was close to the steep portion of the dose-response curve, allowing a marked increase in fluorescence in response to inhibitors.

B) *HTS scatter plot.* EcR:Fpn-GFP cells were treated with 50 ng/ml hepcidin and small molecules for 24h. The results are expressed as normalized Fpn-GFP intensity (ponasterone wells = 100% Fpn-GFP, hepcidin wells = 0% Fpn-GFP). Compounds which caused \geq 60% of the Fpn-GFP signal intensity (green dashed line) were considered possible hits (2.642% compounds). After visual inspection, 14 compounds were confirmed to cause Fpn-GFP retention on the membrane in the presence of hepcidin (0.02% “hit” rate for 70,000 small molecules).

C) *HTS fluorescence images of small molecules identified as hepcidin antagonists.* Shown are cells treated with ponasterone only (“no treatment”), 50 ng/ml hepcidin only, or hepcidin + 10 μ M compounds.

MOL #83428

A1-A8 represent small molecules collectively known as cardiac glycosides, and B1-B3 are potential thiol-modifiers.

Figure 2. The effect of HTS hits on hepcidin-mediated ferroportin degradation, cellular iron export, and hepcidin uptake.

A) Initial validation of HTS hits: dose-response studies. EcR:Fpn-GFP cells were seeded in 384-well plates and induced with 10 μ M ponasterone for 18 h to express Fpn-GFP. Hepcidin (50 ng/ml) was added together with a range of concentrations of fursultiamine, thioxolone or pyrithione zinc for 24 h, and images acquired and analyzed as described for the high-throughput screening. The results are expressed as normalized fluorescence (ponasterone-only =100%, hepcidin-only = 0%). Each point is the mean of 3 replicates and error bars represent standard deviation. The data points were fitted with a 4-parameter logistic curve. EC50 was calculated as the dose causing a midpoint response between minimum and maximum fluorescence for each compound.

B) Secondary validation of HTS hits. The antagonistic effect of fursultiamine (Furs), thioxolone (Thiox), and pyrithione zinc (PyrZn) on hepcidin-mediated Fpn-GFP degradation was analyzed using flow cytometry. The compounds were added at 10 μ M and hepcidin at 100 ng/ml for 24 h. Each bar represents the mean of at least 6 replicates and the error bar is the standard deviation. The results are expressed as normalized fluorescence (ponasterone-only sample=100% Fpn-GFP [dashed line], hepcidin-only sample = 0% Fpn-GFP). * $p < 0.001$.

C) The effect of HTS hits on cellular iron export. Cells were not induced (-Pon) or were induced (+Pon) to express Fpn-GFP for 18 h. Hepcidin (Hep, 100 ng/ml) was then added with or without 10 μ M fursultiamine (Furs) or thioxolone (Thiox). After 24 h, protein lysates were assayed for intracellular ferritin using an ELISA. Pyrithione zinc results are not included because the compound caused significant cellular toxicity. Each bar represents the mean of 3 replicates and error bars represent the standard deviation. Same protein lysates (30 μ g) were analyzed by Western blotting for Fpn-GFP and GADPH.

MOL #83428

D) The effect of HTS hits on ¹²⁵I-hepcidin uptake. Cells induced to express Fpn-GFP were pre-treated with fursultiamine (Furs), pyrrithione zinc (PyrZn), thioxolone (Thiox), or solvent for 30 minutes. ¹²⁵I-hepcidin was then added for 1 hour and cell-associated radioactivity determined using a gamma counter. Each bar represents the mean of 3 replicates and error bar is the standard deviation. *p < 0.05.

Figure 3. Fursultiamine is a potent antagonist of hepcidin-ferroportin interaction.

A) Fursultiamine dose-dependently increases iron export in the presence of hepcidin. Cells expressing Fpn-GFP were incubated for 24h with 100 ng/ml hepcidin and a range of fursultiamine concentrations (0 – 50 μM). Cell lysates were assayed for ferritin. Each data point represents the mean of intracellular ferritin concentrations for at least 6 separate measurements and error bars represent the standard deviation. Because the absolute levels of ferritin differed in individual experiments, the data were normalized within each experiment before they were combined. The normalization was done so that hepcidin-untreated samples had 0% ferritin and hepcidin-treated samples had 100% ferritin. *p = 0.018 and **p < 0.001.

B) Fursultiamine prevents hepcidin-mediated endocytosis of ferroportin. Cells were induced to express Fpn-GFP and were treated with hepcidin (100 ng/ml) and/or fursultiamine (1 or 10 μM) for 30 min. Cells were then biotinylated with nonpermeable primary amine-reactive biotinylation reagent (NHS-PEG₄-biotin), and protein lysates were immunoprecipitated with anti-GFP Ab (ab290). Cell surface Fpn-GFP was detected with streptavidin-HRP. The amount of immunoprecipitated Fpn-GFP was confirmed by Western blotting with anti-GFP Ab (monoclonal mouse).

C) Fursultiamine prevents hepcidin-mediated Fpn-GFP degradation. Cells were induced to express Fpn-GFP and were treated for 24 h with 100 or 250 ng/ml hepcidin and 0, 3, 10, or 30 μM fursultiamine. Protein lysates (30 μg) were immunoblotted with anti-GFP (ab290) to detect Fpn-GFP. The housekeeping protein, GAPDH, was detected by Western blot to verify the amount of protein loaded per lane.

MOL #83428

D) Fursultiamine prevents hepcidin-induced posttranslation modification of ferroportin. Cells were not induced (-Pon) or were induced (+Pon) to express Fpn-GFP. Induced cells were then pre-treated with fursultiamine (0, 10, and 30 μ M) for 1 h and 1 μ g/ml hepcidin added for 20 min. Protein lysates were immunoprecipitated with anti-GFP Ab (ab290) and immunoblotted with anti-poly/monoUb Ab (FK2, top panel) or anti-Fpn Ab R1 (bottom panel).

E) Fursultiamine does not inhibit the endocytosis of LDL receptor. Fpn-GFP expressing cells were treated with a solvent (white bar), a range of fursultiamine concentrations (0.03-10 μ M, grey bars) or with an LXR agonist (1 μ M, black bar) known to decrease LDL uptake. DiI-LDL was added for 30 min and its uptake was quantified using a fluorescence scanner. The data shown represent the mean of at least 6 measurements and the error bars represent the standard deviation.

Figure 4. Molecular mechanism of fursultiamine as a hepcidin antagonist

A) Fursultiamine tightly associates with ferroportin. Cells were induced to express Fpn-GFP and pretreated with solvent (bars 1 and 2) or 10 μ M fursultiamine (bars 3-6) for 1 hour. Cells were then either not washed (co-treatment or "Co-T", black bar) or were washed with PBS 3 times (pre-treatment or "Pre-T", gray bar) and 1 μ g/ml hepcidin added for an additional 1 or 2 h. Amount of Fpn-GFP was quantified using flow cytometry. Each bar represents at least 3 replicates and error bars represent the standard deviation. Results were expressed as normalized amount of Fpn-GFP where hepcidin-untreated sample = 100% and hepcidin-treated (1 or 2 h) sample = 0%.

B) Hepcidin binding to ferroportin is attenuated in the presence of fursultiamine. Cells were induced to express Fpn-GFP, and were pretreated with 0 or 10 μ M fursultiamine (Furs) for 30 minutes. A range of biotinylated hepcidin (B-hep) concentrations (0, 2.5, 5, and 10 μ g/ml) was added to the cells for another 30 minutes. Protein lysates were immunoprecipitated with anti-GFP Ab (ab290), and biotinylated hepcidin bound to Fpn-GFP was detected with streptavidin-HRP. The amount of immunoprecipitated Fpn-GFP was confirmed with anti-Fpn Ab.

MOL #83428

C) *Fursultiamine blocks Fpn residue C326.* Cells expressing Fpn-GFP were treated with either hepcidin (0.5 and 1 $\mu\text{g/ml}$) or fursultiamine (1, 3, 10, and 30 μM) for 30 minutes. Cell surface Fpn-GFP was labeled with maleimide-biotinylation reagent for 30 minutes in 4C. Total protein lysates were immunoprecipitated with anti-GFP Ab (ab290), and samples were analyzed by Western blotting using streptavidin-HRP (top panel) or anti-GFP antibody (bottom panel).

Figure 5. Fursultiamine is a unique and potent hepcidin antagonist.

A) *Principal metabolite of fursultiamine hydrochloride does not act as hepcidin antagonist.* Cells were induced with ponasterone to express Fpn-GFP, and treated for 24 h with 100 ng/ml hepcidin and either fursultiamine or its metabolite thiamine (1-100 μM). Amount of Fpn-GFP was quantified using flow cytometry. Each data point represents 3 replicates and the error bars represent the standard deviation. Results are expressed as %Fpn-GFP where ponasterone-only sample = 100% and hepcidin-treated sample = 0%.

B) *Other thiol-modifying drugs are weak or inactive as antagonists of hepcidin.* Cells were induced to express Fpn-GFP and treated with 100 ng/ml hepcidin and a range of concentrations of fursultiamine, NAC or MESNA. After a 24 h incubation, Fpn-GFP was quantified with flow cytometry. Each data point represents at least 3 replicates and error bars represent the standard deviation.

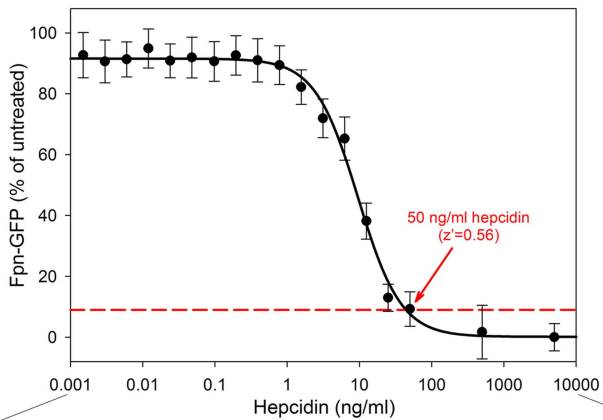
Figure 6. Fursultiamine is not a robust hepcidin antagonist *in vivo*.

A) Mice (n=4/group) were injected intraperitoneally with solvent or 2.5 mg fursultiamine. One hour later, mice were injected with 50 μg hepcidin. Serum iron was analyzed 3 h after hepcidin injection. Bars represent the mean serum iron for each group and error bars represent the standard deviation.

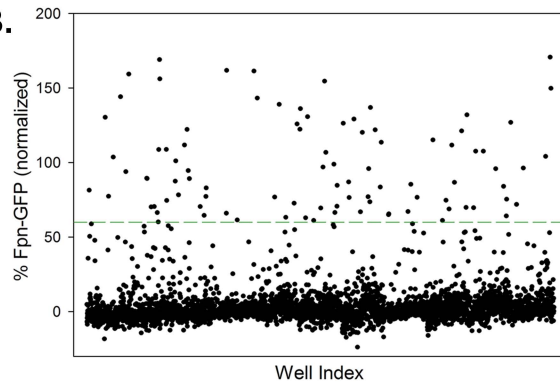
B) Experiment was conducted as in A), but fursultiamine doses ranged from 0.5 to 2 mg.

Figure 1.

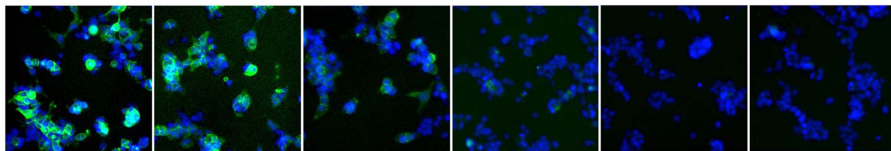
A.



B.



0 0.8 3.1 12.5 50 500



C.

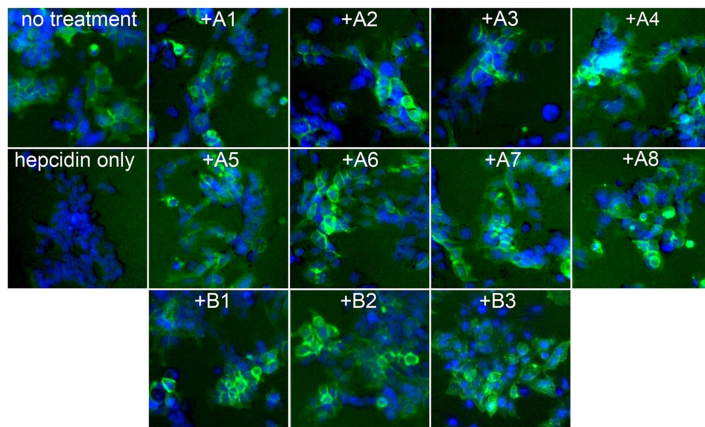


Figure 2.

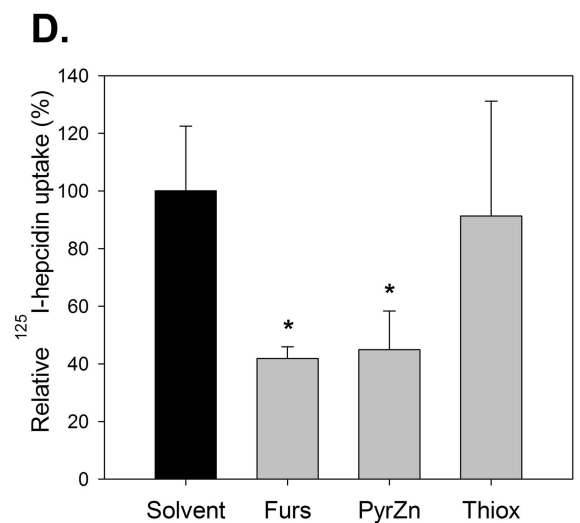
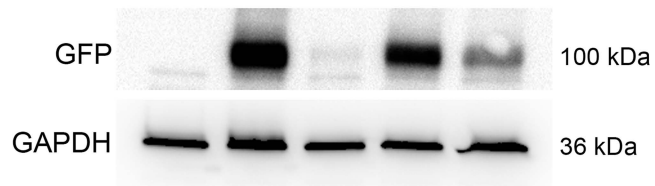
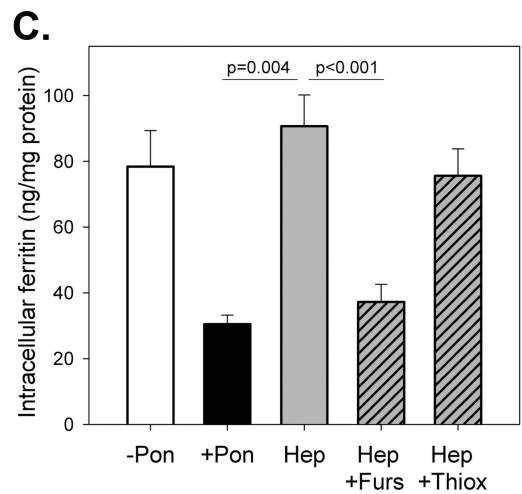
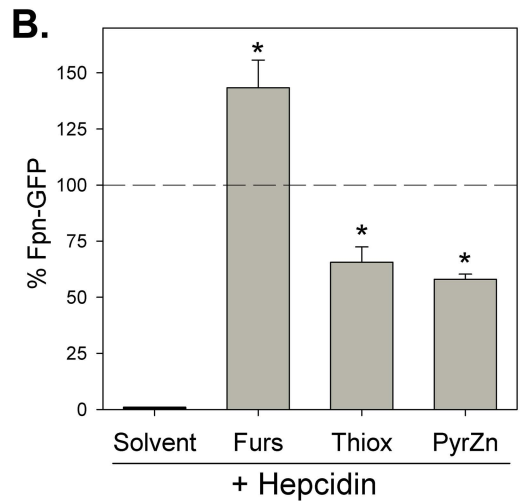
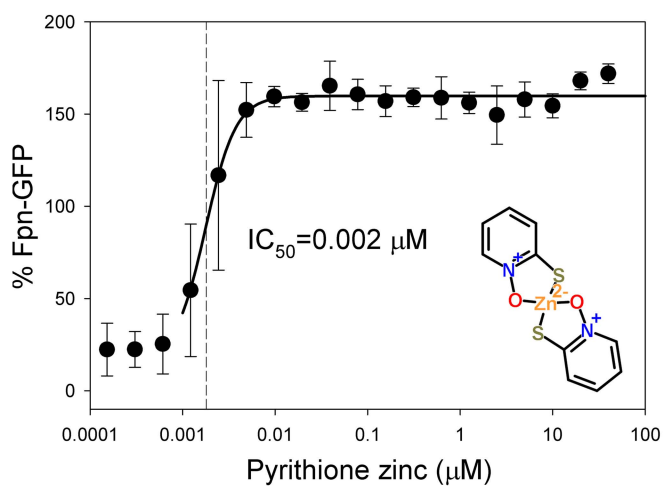
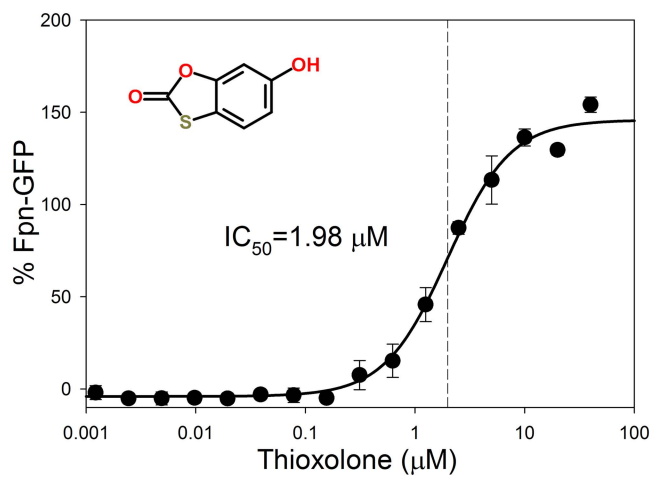
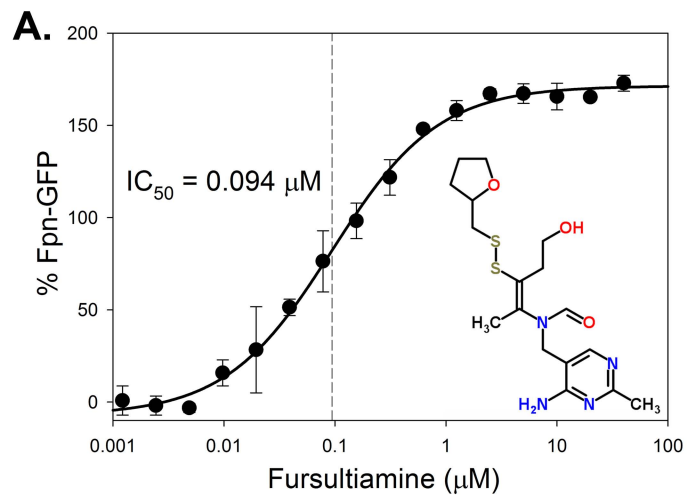


Figure 3.

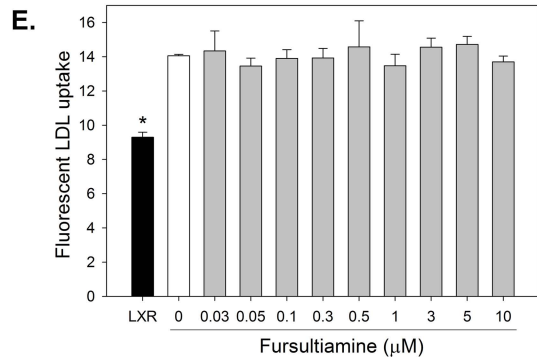
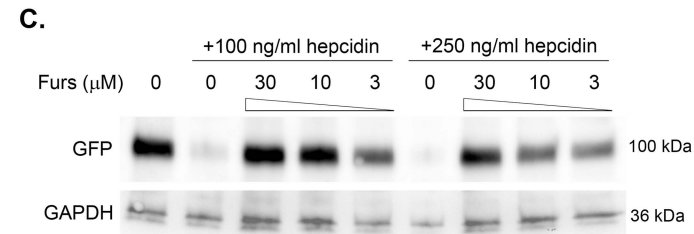
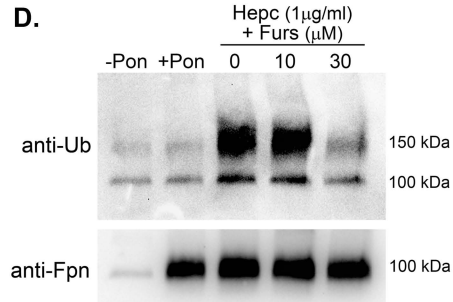
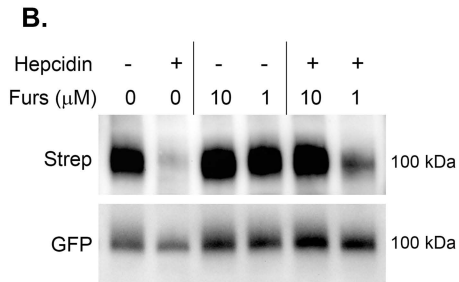
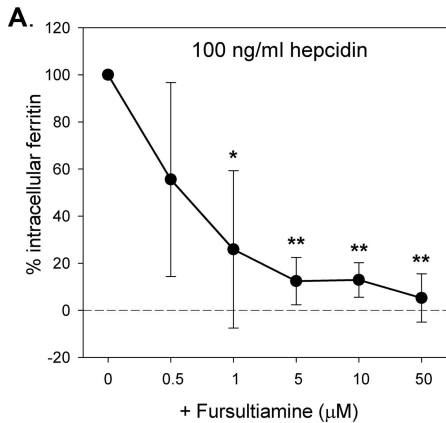


Figure 4.

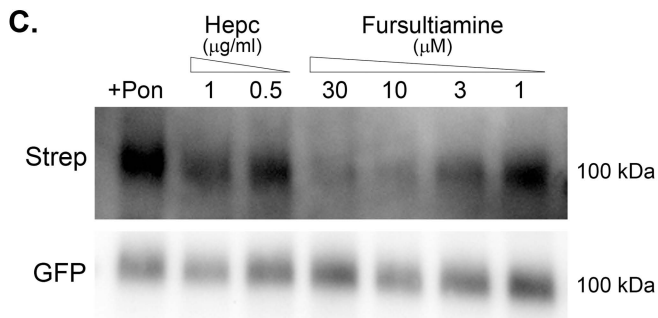
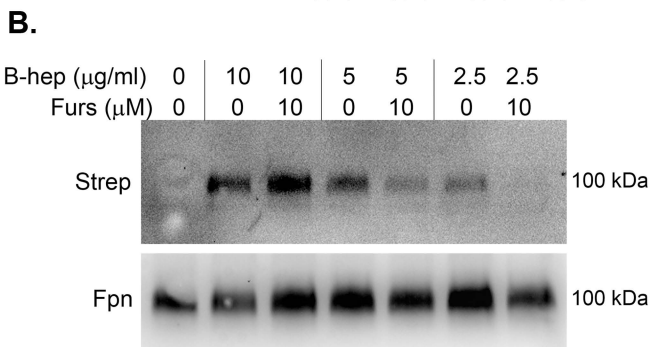
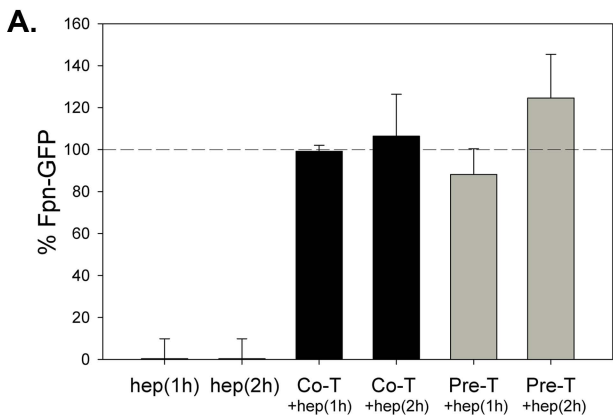


Figure 5.

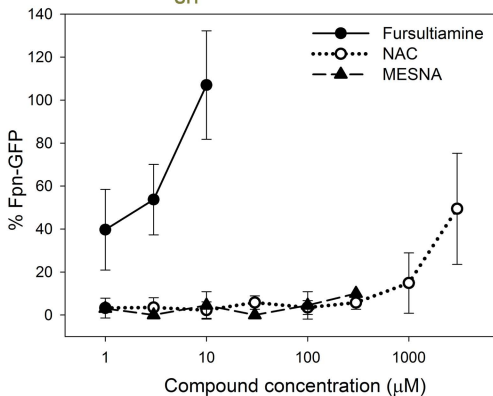
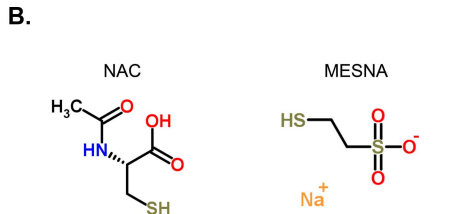
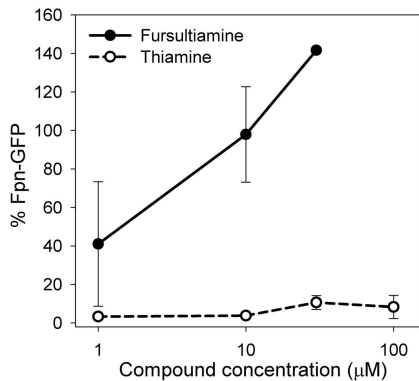
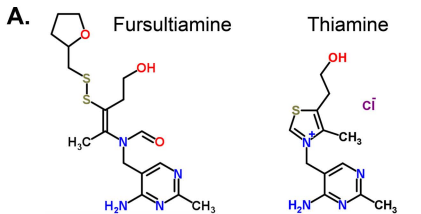


Figure 6.

